ELSEVIER

Polymer 40 (1999) 5285–5296

polymer

Effects of crosslinking on polyaniline films' doping behavior and degradation under weathering

F.T. Liu[a], K.G. Neoh[a,*], E.T. Kang[a], S. Li[a], H.S. Han[b], K.L. Tan[b]

[a]Department of Chemical and Environmental Engineering, National University of Singapore, 10 Kent Ridge Crescent, Singapore 119260, Singapore
[b]Department of Physics, National University of Singapore, 10 Kent Ridge Crescent, Singapore 119260, Singapore

Received 19 October 1998; accepted 27 October 1998

Abstract

The effects of crosslinking on solution cast polyaniline films were investigated by means of X-ray photoelectron spectroscopy, atomic force microscopy, bulk elemental analysis, resistivity and tensile strength measurements. By comparing the anion/N molar ratio at the surface and bulk of the film, it was found that crosslinking of the films retards the dopant infusion process during reprotonation. The extent of doping has a significant effect not only on the film's resistivity, but also its tensile strength. Under simulated weathering, the degradation mechanisms of the non-crosslinked and crosslinked films are similar. As a result of the reactions occurring in the polyaniline chains under simulated weathering, profound changes in the chemical state of the C and N species are evident. In addition to the changes in the film's physical and electrical characteristics, the surface morphology of the films also undergoes substantial changes, especially for the reprotonated crosslinked films. © 1999 Elsevier Science Ltd. All rights reserved.

Keywords: Polyaniline films; Crosslinking; Doping behavior

1. Introduction

The potential of using polyaniline (PAn) in practical applications is substantially enhanced by two important features: the reversible nature of its conductivity [1] and the feasibility of processing the polymer into films or fibers [2,3]. The aniline polymer is usually prepared in aqueous HCl [1], and the resulting conducting polymeric salt is insoluble in common organic solvents. Treatment of the polyaniline salt with a base yields the insulating polyaniline base (50% intrinsically oxidized emeraldine or EM base) which is soluble in *N*-methyl pyrrolidinone (NMP) [4]. Attempts were made to induce processability of polyaniline salts through the use of organic acid dopants, such as camphorsulfonic acid [5], and sulfosalicylic acid (SSA) [6]. We also reported on the physicochemical properties of films cast from polyaniline salt solutions in NMP [7]. Thus, conducting polyaniline films can be obtained by direct casting of certain salt solutions or the subsequent doping (protonation) of the base film cast from NMP solution. One of the major concerns which needs to be addressed is the lack of mechanical strength of the PAn films. The salt films obtained from directing the casting of the salt solutions possess a much lower mechanical strength than the films obtained from reprotonation of the base film. Although a large number of studies [8–13] were devoted to the thermal stability and degradation behavior of PAn, the issue of how the mechanical strength and properties of PAn films change under simulated weathering conditions remains unclear. In the present work, we discuss the enhancement of the mechanical strength of the PAn base films through crosslinking and a comparison of the doping characteristics of the crosslinked and non crosslinked films and their degradation behavior under simulated weathering conditions. The effects of different acid dopants on the reprotonation and degradation processes were also investigated. In particular, the emphasis is on the change in the mechanical and electrical properties, and the loss of the dopants during the weathering tests. The films were characterized by bulk elemental analysis, X-ray photoelectron spectroscopy (XPS) analysis, tensile strength and resistivity measurements.

2. Experimental

2.1. Sample preparation

Polyaniline was synthesized via the oxidative polymerization of aniline with ammonium persulfate in 1 M H_2SO_4

---

* Corresponding author. Tel.: + 65 772 3044; fax: + 65 779 1936.
E-mail address: chenkg@nus.edu.sg (K.G. Neoh)

PII: S0032-3861(98)00758-7

according to the method described in the literature for 1 M HC1 [1]. It was converted to EM base by treatment with excess 0.5 M NaOH for 15 h, followed by washing with water until the filtrate was neutral. The base powder was dried by pumping under reduced pressure. The pristine "non-crosslinked" EM film was prepared by dissolving the EM base powder in NMP solution (6 wt.%). The residual NMP was removed by exhaustive pumping at room temperature. It should be noted that the term "non-crosslinked" is used for convenience, as we have earlier shown that a small amount of crosslinking is introduced even when EM films are cast from dilute NMP solution at room temperature [14]. The crosslinked EM film was prepared by heating an 8 wt.% NMP solution of EM base in an air circulated oven at the temperature of 110°C for 2 h. The solution first formed a gel which eventually led to the formation of a crosslinked EM film [15]. In both the cases, the film's thickness was estimated to be around 10 μm from its area and density.

Reprotonations of the films were carried out by immersing EM base film in 1 M $HClO_4$, toluenesulfonic acid (TSA) or SSA for 24 h. The films were wiped dry, pressed between two pieces of filter paper and then dried under reduced pressure by pumping before being subjected to further characterization.

2.2. Instrumentation

The tensile strength of the polyaniline films of dimension $0.5 \times 1.5\ cm^2$ was measured at room temperature using the Instron model 5544 tensile strength tester. For each tensile strength reported, at least two sample measurements were averaged. Each film was dried by pumping under reduced pressure before the measurements were carried out. The electrical resistivity of all the samples were measured using the standard two-probe technique and the resistivity was thus expressed as Ω/sq.

The aging of the films was carried out in a Ci3000 Xenon Weather-Ometer (Atlas Electric Device Co., Chicago, USA). The weather chamber was maintained at a relative humidity of 60% and a dry bulb temperature and black panel temperature of 35°C and 63°C, respectively. The irradiation directed at the film's surface simulated solar irradiation with an intensity of 0.46 W/m^2 at 340 nm. For each 30-min test, a water spray was activated for 5 min. After varying periods of time, the film was removed from the chamber and dried under reduced pressure before being subjected to analytical and physical tests. The same aging tests were also made under similar irradiation conditions but without the activation of the water spray, to determine the effects of irradiation only.

The analysis of the film by XPS was made on a VG ESCALAB MK II spectrometer with a Mg Kα X-ray source (1253.6 eV photons). The X-ray source was run at a reduced power of 120 W (12 kV and 10 mA). The polymer films were mounted on the standard VG sample studs by means of double-sided adhesive tape. The core-level spectra were obtained at a take off angle of 75°. The pressure in the analysis chamber was maintained at 10^{-8} mbar or lower during the measurements. To compensate for surface charging effects, all binding energies were referenced to the C1s neutral carbon peak at 284.6 eV. In spectral deconvolution, the full width at half maximum of the peak components of a spectrum was kept a constant. Surface chemical compositions were determined from peak area ratios corrected with the appropriate experimentally determined sensitivity factors, and are accurate to $\pm 10\%$.

For the elemental bulk analysis, the C, H, N and S contents were measured using the Perkin-Elmer Series II elemental analyzer. Cl content was analyzed by the following procedure: the sample was combusted and any chlorine gas evolved was absorbed into a solution containing 2 ml of 0.2 N NaOH, 1 ml of H_2O_2 and 10 ml of deionized water in a 500 ml Schonigen flask. The amount of chlorine was then determined by titration with mercuric nitrate ($Hg(NO_3)_2$) using 0.1% diphenyl carbazone as indicator.

The atomic force microscopy (AFM) measurements were carried out using a Nanoscope III scanning force microscope. All images were collected in air under a constant force mode (scan size 5.0 μm, set point 3.34 V, scan rate 0.5 Hz).

3. Results and discussion

3.1. Non-crosslinked films

The non-crosslinked EM film freshly prepared under reduced pressure without heating can be redissolved in NMP to a large extent and is also amorphous [15]. The complete removal of NMP in the as-cast EM film cannot be achieved easily and some NMP is retained in the film which acts as a plasticizer. The residual NMP in the film can also promote crosslinking in the EM film by first forming hydrogen bonds with NH groups of PAn [16]. When the EM base film is reprotonated by acids, the C=O groups of NMP may also interact via hydrogen bonding with the acids and this may weaken the interchain interaction.

The reprotonation of EM base film by $HClO_4$ and TSA results in a rapid colour change from the original purplish blue to dark green. The SSA-treated EM base film, however, retains the brownish tint of the EM base even after treatment for 24 h. Thus, from the visual observation it is clear that the EM base films have undergone different degrees of protonation. This can be attributed to the increasing difficulty for the bigger anions to penetrate into the bulk of the films which results in vastly different resistivities of the reprotonated EM films. The $HClO_4$-treated EM film is the most conductive with the resistivity of the order of 10^3 Ω/sq.; the TSA- and SSA-treated EM films are less conductive with resistivity values of the order of 10^4 and 10^5 Ω/sq., respectively (Fig. 1(a), values at aging time = 0 h).

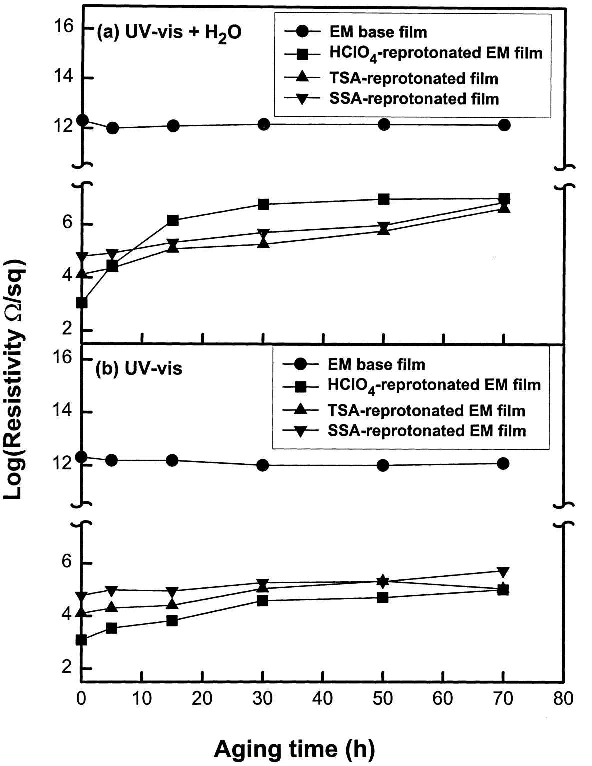

Fig. 1. Resistivity of non-crosslinked EM base film and reprotonated films as a function of aging time under (a) simulated weathering (UV-vis + H_2O); (b) UV-vis irradiation only.

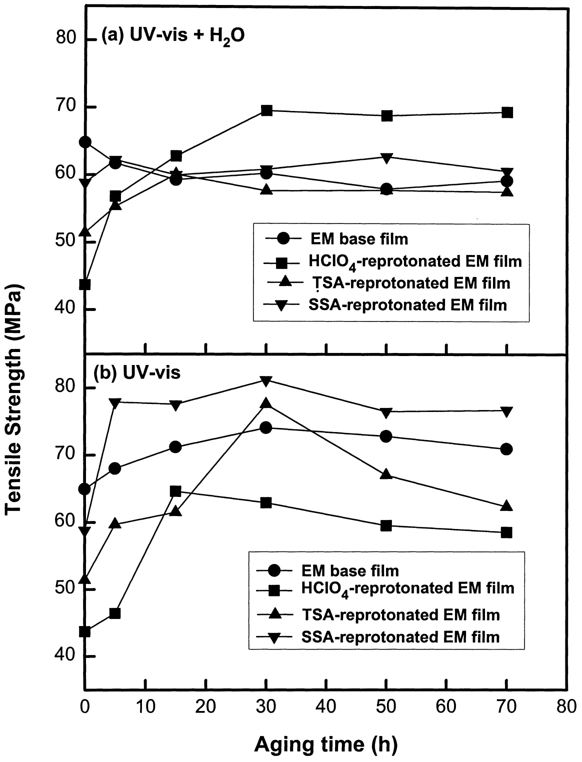

Fig. 2. Tensile strength of non-crosslinked EM base film and reprotonated films as a function of aging time under (a) simulated weathering (UV-vis + H_2O); (b) UV-vis irradiation only.

The reprotonation of the base film results in a decrease of the film's tensile strength. The EM base film has a tensile strength of 64.8 MPa and this value drops to 43.7, 51.4 and 58.8 MPa for films reprotonated by $HClO_4$, TSA and SSA, respectively (Fig. 2, values at aging time $= 0$ h). Thus, the tensile strength decreases in the same order as the decrease in the film resistivity. This is consistent with the migration of the dopants into the bulk of the film and the weakening of interchain interactions as discussed earlier.

The XPS N1s core-level spectra of the EM base film before and after reprotonation by $HClO_4$, TSA and SSA are shown in Figs. 3(a)–(d), respectively. The N1s core-level spectrum in Fig. 3(a) can be curve-fitted with two major components with binding energy (BEs) at about 398.2 and 399.4 eV, attributable to the imine (–N=) and amine (–NH–) nitrogens, respectively [17–19]. The residual high BE components above 400 eV may have resulted, at least in part, from surface oxidation products or weakly charge transfer complexed oxygen species [17]. This assignment is consistent with the presence of a weak O1s core-level signal in most EM base samples. The N1s spectra of the EM films after reprotonation by $HClO_4$, TSA and SSA (Figs. 3(b), (c) and (d) are not exactly similar. The high-BE tail attributed to the N^+ components was resolved as the two peaks, separated by 1.45–1.50 and 2.95–3.10 eV from the amine peak respectively. The degrees of protonation as calculated from the N^+/N ratios in these reprotonated films are given in Table 1. The difference in the lineshapes of the reprotonated films probably arises from the distribution of the positive charges. We postulated that positive charges more localized in a bipolaron-type defect structure would result in a N1s lineshape different from the corresponding spectrum when a polaron lattice is present [20].

The XPS C1s core-level spectra of EM base film and its reprotonated EM film are shown in Figs. 4(a)–(d), respectively. The major feature of the core-level spectra is a peak at 284.6 eV, characteristic of the neutral carbon species, viz., C–H, C–C and C–N species, in the backbone of the polymer. The small high-BE tail in the Cls core-level spectrum can be deconvoluted into three peaks with BEs at around 286.2, 287.9, and 288.7 eV, which are ascribed to the C–O, C=O, and O–C=O group, respectively [21]. In the case of the SSA-reprotonated films, the SSA also contributes to the COOH component intensity (Fig. 4(d)).

The XPS analysis gives the composition in the surface region (<10 nm) of the films only. From Table 1, it can be seen that all the –N= units at the surface of the EM film are reprotonated by $HClO_4$, TSA and SSA and a high degree of reprotonation was achieved in all these cases. However, from visual observations and resistivity measurements, it is clear that the degree of migration of the dopant anions into the bulk of the film is highly dependent on the size of the anions. The bulk elemental analysis results in Table 2 shows that the Cl/N ratio of $HClO_4$-reprotonated film is

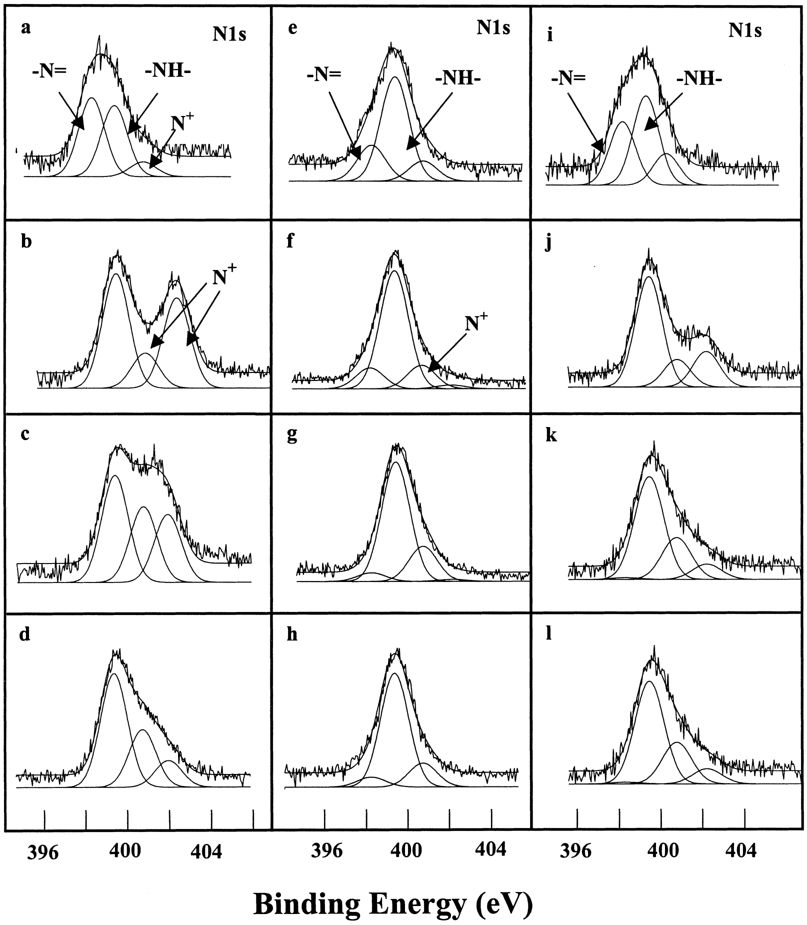

Fig. 3. XPS N1s core-level spectra of (a)–(d) non-crosslinked EM base film and the films reprotonated by $HClO_4$, TSA and SSA, respectively; (e)–(h) the respective films after simulated weathering (UV-vis + H_2O) for 50 h; (i)–(l) the respective films after UV-vis irradiation only for 50 h.

0.52, which is very similar to the surface Cl/N ratio (0.50 in Table 1). This implies that the bulk of the film is also largely protonated unlike the reprotonation of the much thicker films (150 μm in thickness) by HCl reported earlier [16]. In contrast, the low bulk S/N ratio (0.01) of the SSA-reprotonated film confirms that the reprotonation is only limited to the surface region. The TSA reprotonated film with a bulk S/N mole ratio of 0.09 represents an intermediate situation between the $HClO_4$ and SSA reprotonated films.

Table 1
Surface compositions of reprotonated non-crosslinked EM films under simulated weathering (UV-vis + H_2O) and UV-vis irradiation only (UV-vis)

Sample	Aging condition	Surface composition							
		−N=/N	−NH/N	N^+/N	Cl or S/N	C/C_T[a]	C–O/C_T	C=O/C_T	O–C=O/C_T
EM	Pristine	0.48	0.42	0.10	0	0.89	0.09	0.02	0
	UV-vis + H_2O, 50 h	0.22	0.65	0.13	0	0.71	0.20	0.05	0.04
	UV-vis, 50 h	0.35	0.47	0.18	0	0.80	0.14	0.03	0.03
$HClO_4$-EM	Pristine	0	0.51	0.49	0.50	0.73	0.21	0.03	0.03
	UV-vis + H_2O, 50 h	0.08	0.72	0.20	0.05	0.63	0.25	0.08	0.04
	UV-vis, 50 h	0	0.64	0.36	0.24	0.66	0.24	0.04	0.06
TSA-EM	Pristine	0	0.41	0.58	0.55	0.78	0.18	0.03	0.01
	UV-vis + H_2O, 50 h	0.04	0.72	0.24	0.07	0.63	0.25	0.07	0.05
	UV-vis, 50 h	0.03	0.63	0.35	0.22	0.70	0.18	0.06	0.06
SSA-EM	Pristine	0	0.56	0.44	0.38	0.67	0.23	0.05	0.05
	UV-vis + H_2O, 50 h	0.05	0.77	0.19	0.06	0.60	0.26	0.08	0.06
	UV-vis, 50 h	0	0.64	0.31	0.25	0.66	0.22	0.05	0.07

[a] Represents fraction of carbon not bonded to oxygen, such as C=C, C–N, C–H.

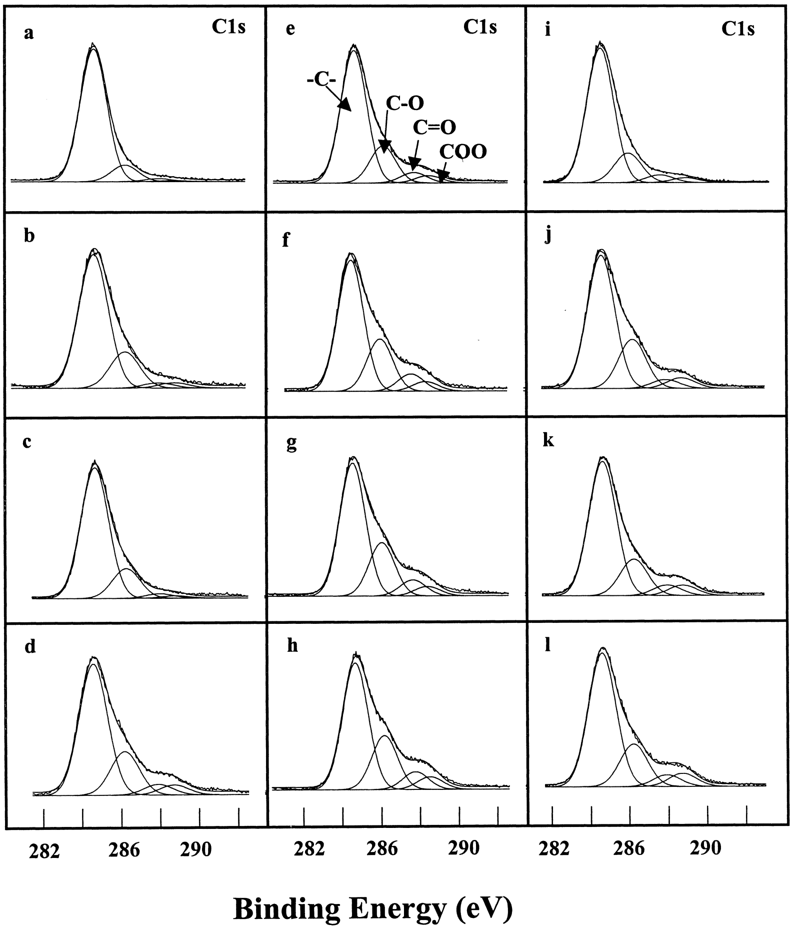

Fig. 4. XPS C1s core-level spectra of (a)–(d) non-crosslinked EM base film and the films reprotonated by $HClO_4$, TSA and SSA, respectively; (e)–(h) the respective films after simulated weathering (UV-vis + H_2O) for 50 h; (i)–(l) the respective films after UV-vis irradiation only for 50 h.

Under simulated weathering, the resistivity of the EM base film remains almost unchanged while the resistivities of the $HClO_4$-, TSA- and SSA-reprotonated films increase to $> 10^6$ Ω/sq. after 70 h (Fig. 1(a)). The largest increase is observed in the most conductive film, the $HClO_4$-reprotonated film. The tensile strength of the EM base film shows a slight decrease with weathering whereas the tensile strengths of the reprotonated films show an increase, with the largest increase observed in the $HClO_4$-reprotonated film (Fig. 2(a)). The increase in resistivity and tensile strength of the reprotonated films are linked to the loss of dopant from these films as can be seen by the decrease in the bulk Cl/N or S/N ratio in Table 2. After 50 h of simulated weathering (data denoted by UV-vis + H_2O, 50 h in Table 2), the amount of dopant in the bulk decreased almost by a factor of 2 in the $HClO_4$-reprotonated film, and the dopant/N ratio is no longer significant for the TSA and SSA-reprotonated films. The C/N ratio remains close to 6 for all the films after 50 h of simulated weathering. It is interesting to note that the tensile strength of the $HClO_4$-reprotonated film after 20 h of simulated weathering increased to a value higher than that of the pristine EM base. This increase in tensile strength is attributed to the increase in crosslinking effects promoted perhaps by the residual NMP in the film as it undergoes deprotonation. In an earlier work, we reported that the EM base films cast from NMP become significantly less soluble in NMP after each reprotonation–deprotonation cycle [22]. After 70 h of simulated weathering, the tensile

Table 2
Bulk composition of non-crosslinked films before and after simulated weathering (UV-vis + H_2O) and UV-vis irradiation (UV-vis)

Sample	Aging condition	Elemental composition		
		C/N	H/N	Cl or S/N
$HClO_4$-EM	Pristine	6.1	7.7	0.52
	UV-vis + H_2O, 6 h	6.0	6.8	0.25
	UV-vis + H_2O, 50 h	5.9	6.5	0.23
	UV-vis, 50 h	5.8	4.7	0.26
TSA-EM	Pristine	6.6	6.8	0.09
	UV-vis + H_2O, 6 h	6.0	5.8	0.01
	UV-vis + H_2O, 50 h	6.1	6.0	0.007
	UV-vis, 50 h	6.0	6.0	0.03
SSA-EM	Pristine	5.8	5.8	0.01
	UV-vis + H_2O, 6 h	5.9	5.1	0.005
	UV-vis + H_2O, 50 h	5.6	5.4	0.005
	UV-vis, 50 h	5.9	5.2	0.006

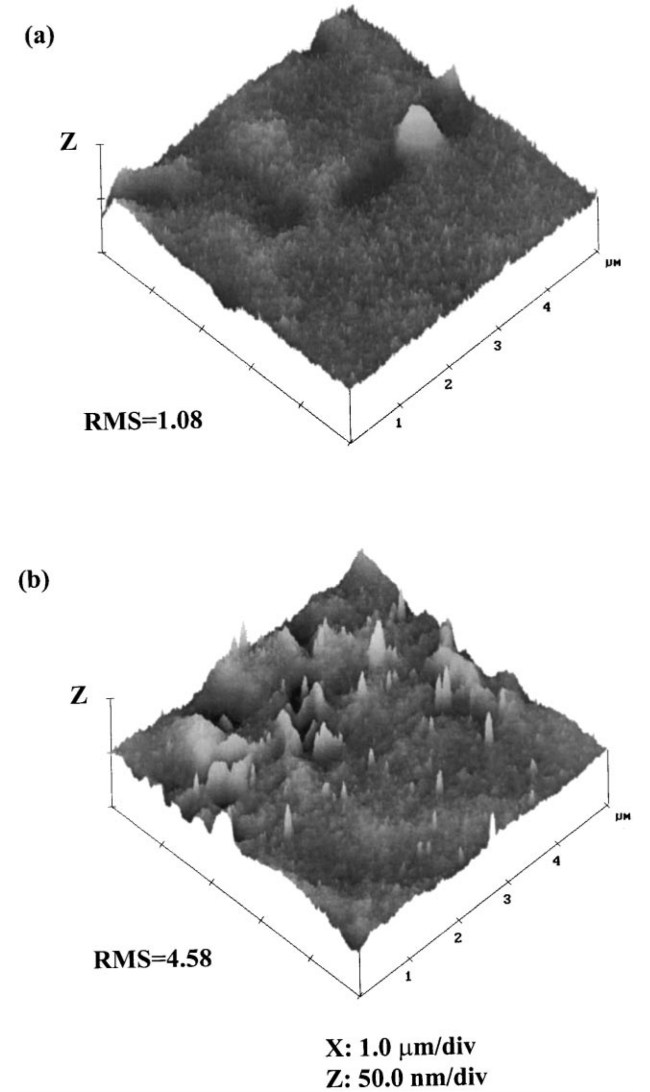

Fig. 5. AFM images of non-crosslinked EM film: (a) pristine and (b) after simulated weathering (UV-vis + H_2O) for 50 h.

strengths of the TSA- and SSA-reprotonated films also increase but are lower than that of the $HClO_4$-reprotonated film, and are rather similar to that of EM base. The degrees of reprotonation achievable in the bulk of the TSA- and SSA-reprotonated films are substantially less than that of $HClO_4$-reprotonated film. Thus, the subsequent increase in crosslinking upon deprotonation of the former during simulated weathering is also expected to be substantially less, as can be seen from Fig. 2(a).

The XPS N1s core-level spectra of EM base and its reprotonated films after 50 h of simulated weathering are shown in Figs. 3(e)–(h), respectively. The EM base film shows an increase of amine species and a decrease of imine components (Fig. 3(e) and Table 1). The result implies that the surface has undergone reduction. The reduction of the EM base film surface is probably associated with the hydrolysis reaction [23] which can reduce the imine units to the amine units. The reduction process is substantially enhanced in the presence of the near-UV light illumination [24]. The $HClO_4$-, TSA- and SSA-reprotonated EM films undergo a decrease in the proportion of N^+ species. The process is accompanied by a small increase in the imine component and a substantial increase in amine component (Figs. 3(f)–(h)). This phenomenon is unlike the deprotonation of EM salt films by a base where the decrease in N^+ will result predominantly in the recovery of imine units [18]. However, it was observed that when EM salt loses dopant anions when treated with water, the N^+ species do not just revert to imine species but also to amine species as well [25].

The C1s core-level spectra of the EM base and reprotonated EM film show that an increase in oxidized C species is obtained after simulated weathering (Figs. 4(e)–(h)) and Table 1). Thus, while the intrinsic oxidation state of the polyaniline decreases as indicated by the increase in the proportion of amine groups, the ring C gets oxidized. A similar phenomenon was observed when EM films are exposed to O_3 [26]. We postulate that simulated weathering conditions result in a significant number of carbonyl, hydroxyl and hydroxyl peroxides species being formed which may react with the nitrogen atoms and may also undergo charge-transfer interactions with the nitrogen atoms resulting in N^+ species. This explains why the N^+/N ratio of the films after simulated weathering is significantly higher than the anions (ClO_4^- or $-SO_3^-$)/N ratio (Table 1). An earlier study of the effects of simulated weathering on PAn thin films (1–2 µm thick) showed that N^+/N ratio decreases for one sample while in another sample, the ratio increases with weathering (from 0 to 8 h to 25 days) [27]. While no reason was given for this apparent discrepancy, the authors proposed that the oxidation of amine site produces a protonated imine structure.

The three-dimensional AFM image of pristine non-crosslinked EM film shows a relatively smooth surface with root mean square (RMS) roughness value of 1.08 nm (Fig. 5(a)). This is in agreement with the earlier SEM result and postulate that the interactions between NMP and EM base film can lead to a more isotropic morphology [16]. After simulated weathering for 50 h, this film surface becomes much coarser, with a roughness value of 4.58 nm, as shown in Fig. 5(b). The difference in the surface morphology can be attributed to the changes in surface composition during the simulated weathering arising from oxidation of the polymer backbone and possibly the loss of NMP from the surface region of the film. The extraction of NMP from EM base film by THF was shown to result in a fibrilar morphology [16]. The AFM image of the $HClO_4$-reprotonated film is shown in Fig. 6(a). The more wrinkled surface and higher roughness value of 1.68 nm, compared to that of the EM base film is again attributed to the extraction of NMP from the surface region of the film by $HClO_4$ and the resultant weakened H-bond interaction between the NMP and PAn. After simulated weathering for 50 h, the roughness value of this film increases to 5.17 nm (Fig. 6(b)) as the film

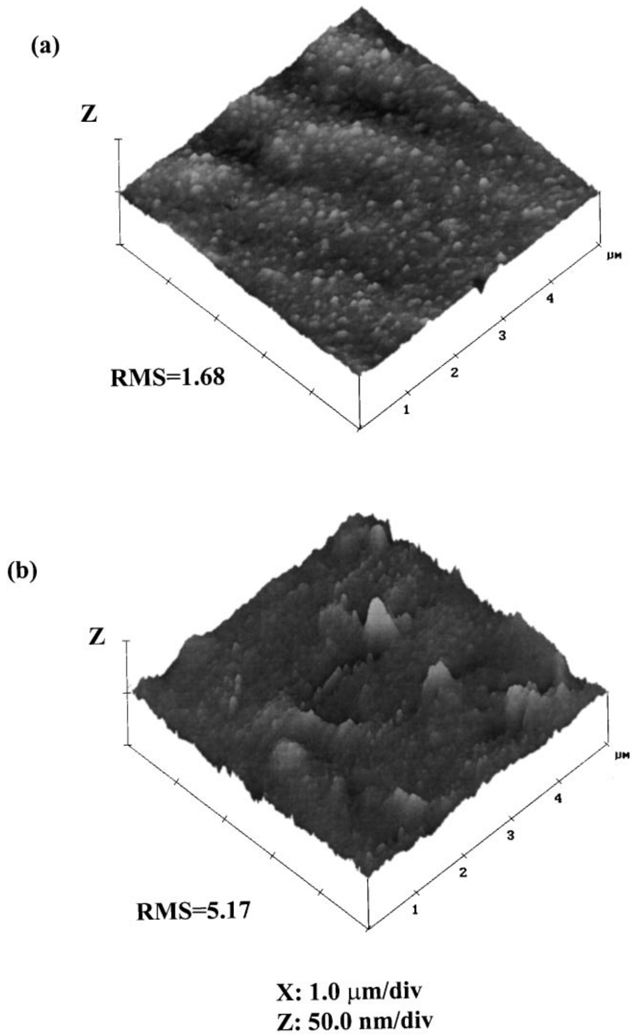

Fig. 6. AFM images of $HClO_4$-reprotonated non-crosslinked EM film: (a) pristine and (b) after simulated weathering (UV-vis + H_2O) for 50 h.

undergoes deprotonation and oxidation of the ring in the polymer backbone.

Under UV-vis irradiation only (without the activation of the water spray), the resistivity of the EM base film also remains unchanged (Fig. 1(b)). The increase in resistivity of the reprotonated films is less than that observed under simultaneous UV-vis irradiation and water spray. The tensile strength of all four types of film increases at first with UV-vis irradiation, then decreases with longer aging time (Fig. 2(b)). The initial increase in tensile strength can probably be attributed to the residual NMP in the films which promotes interchain crosslinking under UV-vis irradiation. For the reprotonated films, the loss of dopants from the bulk of film further promotes this effect. It is interesting to note that, with the exception of the $HClO_4$-reprotonated film, the tensile strengths of the other films under UV-vis irradiation were higher than those of the films under simulated weathering. In the presence of water, the NMP and anions are extracted from the films relatively rapidly and the crosslinking reactions do not proceed after an initial period. By contrast, in the absence of the water spray, the crosslinking reactions may continue for an extended period. However, in the case of the $HClO_4$-reprotonated film, as the bulk of the film is also protonated, the film is weaker than the TSA and SSA reprotonated films. Without the water spray, the ClO_4^- anions are not readily removed from the bulk of the film and so the tensile strength remains lower than those of the EM base film and the TSA and SSA reprotonated films. It should be mentioned that even in the absence of the water spray, the humidity in the test chamber is sufficiently high that some water condensation on the films is observed.

The XPS N1s core-level spectra of EM base and its reprotonated films after 50 h of UV-vis-irradiation are shown in Figs. 3(i)–(l), respectively. The decrease in the proportion of the imine species and the corresponding increase in the amount of the amine component in the EM base film (Fig. 3(i), and Table 1) indicate that the extent of reduction of the surface of EM film is significantly less than those resulted under simulated weathering in the presence of a water spray (Fig. 3(e) and Table 1). For the films reprotonated by $HClO_4$, TSA and SSA, a decrease in N^+species and a corresponding increase in amine components are observed (Figs. 3(j)–(l), Table 1). For these films, the N^+/N ratio remains larger than 0.30 and the anion/N ratio is between 0.22 and 0.25 (Table 1). Thus, these films remain reprotonated to a significant extent and no “free” imine groups are observed, unlike the corresponding cases under simulated weathering. The loss of anions from the bulk of the film is best illustrated by the $HClO_4$-reprotonated film. After 50 h of UV-vis irradiation, the bulk Cl/N ratio is half of the original value (Table 2). In the case of simulated weathering, the same magnitude of decrease is observed after only 6 h (Table 2), indicating the more adverse effects of UV-vis irradiation and water acting in combination. All samples under UV-vis irradiation show the oxidation of the ring C as evidenced by the increase of species such as C–O, C=O, O–C=O (Table 1). Again, in all cases, the extent of ring oxidation under UV-vis irradiation is clearly less than that observed under UV-vis irradiation in combination with an intermittent water spray.

3.2. Crosslinked films

The crosslinked EM base film is insoluble in NMP, but it swells slightly in this solvent. The reprotonation of crosslinked EM base film by $HClO_4$ and TSA also results in a color change from the original purplish blue to dark green. However, this color change is slower than that of non-crosslinked EM base film during the reprotonation process. The crosslinked EM film after SSA protonation retains the purplish brown color of the EM base film. Thus, from the visual observation, it is also clear that the crosslinked EM base film has undergone different degrees of protonation. The $HClO_4$- and TSA-reprotonated crosslinked films with

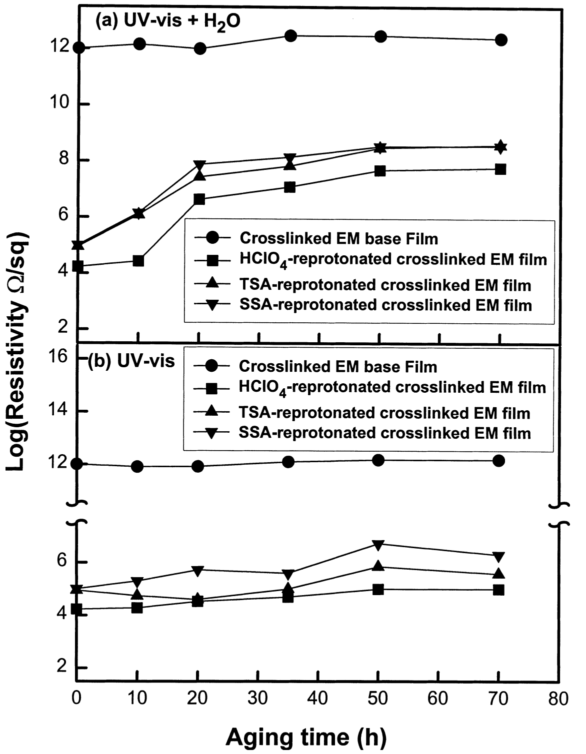

Fig. 7. Resistivity of crosslinked EM base film and reprotonated films as a function of aging time under (a) simulated weathering (UV-vis + H_2O); (b) UV-vis irradiation only.

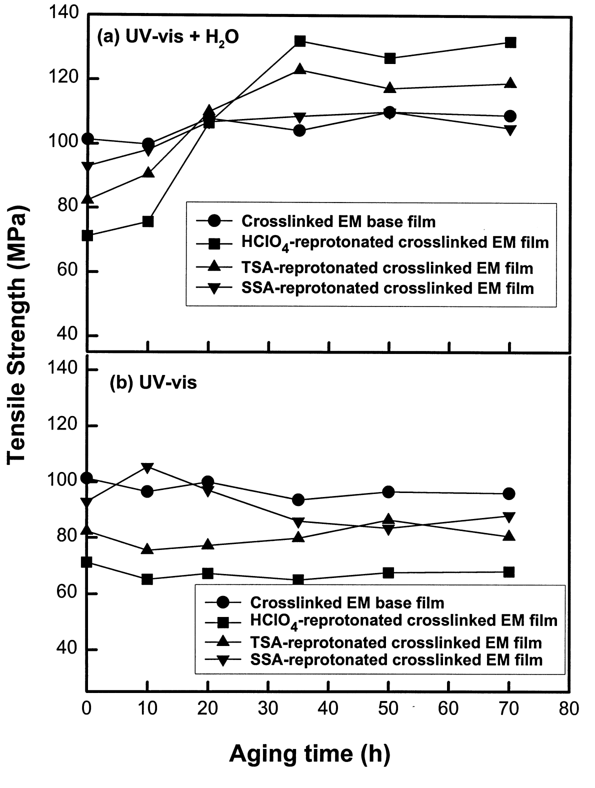

Fig. 8. Tensile strength of crosslinked EM base film and reprotonated films as a function of aging time under (a) simulated weathering (UV-vis + H_2O); (b) UV-vis irradiation only.

resistivities of the order of 10^4 and 10^5 Ω/sq., respectively (Fig. 7(a), values at aging time = 0 h) are ten times less conductive than the same acid-reprotonated non-crosslinked films (Fig. 1(a), values at aging time = 0 h). This can be attributed to the increased difficulty for the anions to penetrate into the crosslinked structure of the film. The SSA-reprotonated crosslinked film has the same surface resistivity as the TSA-treated film (resistivity of the order 10^5 Ω/sq.) even though the visual appearance of the two films is different. It will be shown later, however, that the bulk anion/N ratios of these films are different. The reprotonation of the crosslinked film also results in a decrease of the film's tensile strength, similar to the effect observed with the non-crosslinked film. The crosslinked EM base film has a tensile strength of 103.1 MPa and this value drops to 71.2, 82.3 and 92.9 MPa for the films reprotonated by $HClO_4$, TSA and SSA respectively (Fig. 8(a), values at aging time = 0 h). The decrease in tensile strength is again in the same order as the extent of ion migration into the bulk of the film (see later). However, the tensile strength of the acid-treated crosslinked films is still higher than that of non-crosslinked EM base film (Fig. 2(a)). It should be pointed out that the tensile strength of the crosslinked EM base film is about a factor of 2 higher than that reported earlier for unstretched crosslinked EM base [15]. This difference is attributed to the different extents of crosslinking as the concentration of EM base and temperature used in the present work is significantly different from the values reported earlier. It was shown in our earlier work [21] that heating during the formation of EM base films from NMP solutions, as well as the EM base concentration, has a significant effect on the tensile strength of the resultant films.

The XPS N1s core-level spectra of the crosslinked EM base film before and after reprotonation by $HClO_4$, TSA and SSA are shown in Figs. 9(a)–(d), respectively. The imine (–N=) and amine (–NH–) components at 398.2 and 399.4 eV of the crosslinked EM base film (Fig. 9(a)) are almost identical in intensity, indicating that there is no difference in the oxidation state between the crosslinked and non-crosslinked films (Fig. 3(a)). After reprotonation by $HClO_4$, TSA and SSA, the N1s spectra of the films (Figs. 9(b), (c) and (d)) show that all the imine units are converted to N^+ and the degree of the protonation as calculated from the N^+/N ratios in these reprotonated films are given in Table 3. The anion/N ratios calculated from the peak area ratios of either ClO_4^- or $-SO_3^-$ to N (after correction with the sensitivity factors) are in good agreement with the N^+/N ratio. Although the N^+/N ratios of the reprotonated non-crosslinked and crosslinked films (shown in Tables 1 and 3, respectively) are not substantially different, the resistivities of the crosslinked films are one order of magnitude higher. Thus, the surface N^+/N ratio as determined by XPS does not provide a good indication of the film's conductivity. The formation of any physical or chemical crosslinks in the film is likely to affect the closeness and orientation of the polymer chains which in turn affect the interchain conductivity.

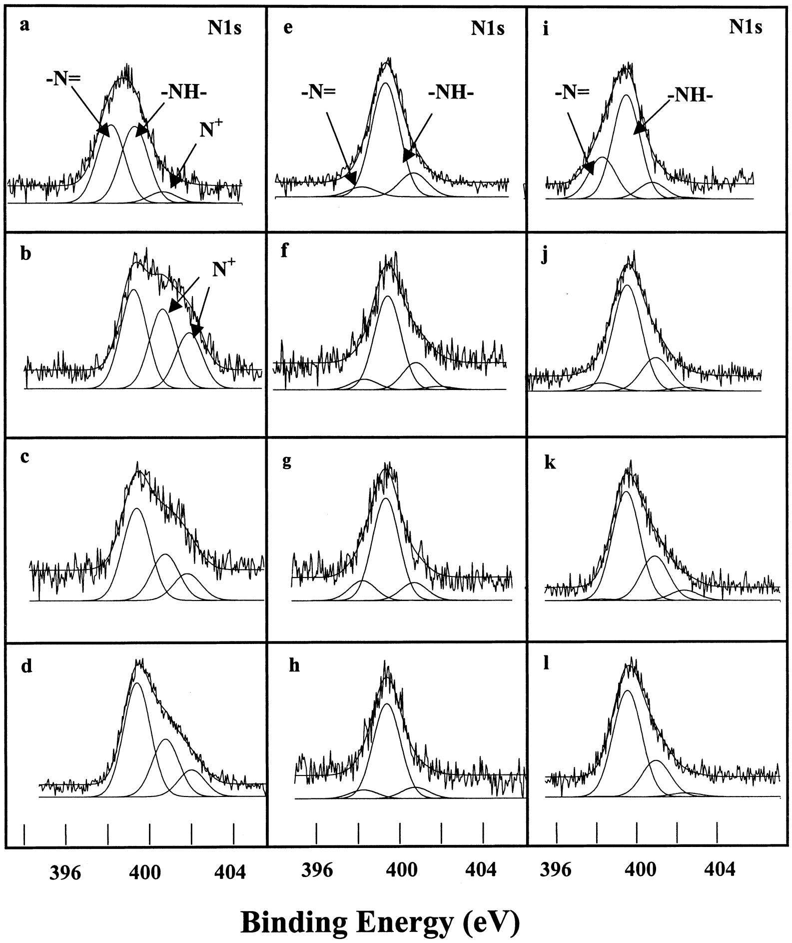

Fig. 9. XPS N1s core-level spectra of (a)–(d) crosslinked EM base film and the films reprotonated by $HClO_4$, TSA and SSA, respectively; (e)–(h) the respective films after simulated weathering (UV-vis + H_2O) for 50 h; (i)–(l) the respective films after UV-vis irradiation only for 50 h.

The bulk analysis results in Table 4 show that the C1/N ratio of the $HClO_4$-reprotonated film is 0.30, which is lower than the surface C1/N ratio (0.52 in Table 3), unlike the $HClO_4$-reprotonated non-crosslinked film in which the surface and bulk C1/N ratios are almost identical (Tables 1 and 2). This result suggests that the $HClO_4$ molecules encounter more difficulty penetrating into the bulk of the crosslinked EM film. As discussed earlier, the TSA and SSA anions have difficulty migrating into the bulk of the non-crosslinked films, and for the crosslinked films, the problem is further accentuated. A comparison of the $-SO_3^-$/N ratios of these films in Tables 3 and 4 shows that there is minimal reprotonation in the bulk of the film, especially for the SSA treated films, even though the surface N^+/N ratio (determined by XPS) is 0.42.

Under simulated weathering (UV-visible irradiation and water spray), the resistivity of the crosslinked EM base film remains almost unchanged, while the resistivities of the $HClO_4$-, TSA- and SSA-reprotonated films increase by three orders of magnitude after 70 h (Fig. 7(a)). The tensile strength of the crosslinked EM base film does not show much variation with weathering, whereas the tensile strengths of the crosslinked films after reprotonation increase to a value even higher than that of the pristine crosslinked EM film before showing a decrease (Fig. 8(a)). The increase in tensile strength of the crosslinked films after reprotonation promoted by the loss of dopants during weathering demonstrate that the extent of crosslinking can be further enhanced beyond the level initially achieved via thermal treatment of the EM base gel.

The XPS N1s core-level spectra of crosslinked EM and its reprotonated films after 50 h of simulated weathering are shown in Figs. 9(e)–(h), respectively. The crosslinked EM base film shows an increase in the amount of amine species and a decrease in imine components (Fig. 9(e) and Table 3). These results imply that the surface has undergone reduction, similar to the results of the non-crosslinked EM base film. For the films reprotonated by $HClO_4$, TSA and SSA, a decrease in the proportion of N^+ species is accompanied by a small increase in the imine components and a substantial increase of amine components (Figs. 9(f)–(h)). These changes in surface composition are again similar to those of non-crosslinked films. A comparison of the C1s core-level spectra of the crosslinked EM base film and the

Table 3
Surface compositions of reprotonated crosslinked EM films under simulated weathering (UV-vis + H_2O) and UV-vis irradiation only (UV-vis)

Sample	Aging condition	Surface composition							
		–N=/N	–NH/N	N^+/N	C1 or S/N	C/C_T[a]	$C–O/C_T$	$C=O/C_T$	$O–C=O/C_T$
EM	Pristine	0.47	0.46	0.07	0	0.82	0.14	0.03	0.01
	UV-vis + H_2O, 50 h	0.24	0.65	0.11	0	0.63	0.25	0.08	0.04
	UV-vis, 50 h	0.25	0.63	0.10	0	0.79	0.15	0.04	0.02
$HClO_4$-EM	Pristine	0	0.41	0.58	0.52	0.75	0.20	0.02	0.03
	UV-vis + H_2O, 50 h	0.04	0.73	0.23	0.08	0.67	0.23	0.06	0.04
	UV-vis, 50 h	0.02	0.70	0.27	0.10	0.70	0.22	0.03	0.05
TSA-EM	Pristine	0	0.50	0.50	0.50	0.84	0.13	0.01	0.01
	UV-vis + H_2O, 50 h	0.06	0.73	0.22	0.10	0.69	0.21	0.06	0.04
	UV-vis, 50 h	0	0.66	0.34	0.16	0.78	0.14	0.04	0.04
SSA-EM	Pristine	0	0.58	0.42	0.36	0.77	0.17	0.03	0.03
	UV-vis + H_2O, 50 h	0.07	0.82	0.10	0.10	0.67	0.20	0.06	0.07
	UV-vis, 50 h	0	0.72	0.28	0.10	0.74	0.18	0.03	0.05

[a] Represents fraction of carbon not bonded to oxygen, such as C=C, C–N, C–H.

reprotonated films before and after simulated weathering (Fig. 10 and Table 3) show an increase in oxidized C species as a result of weathering. Thus, the XPS results show that the surface degradation of the crosslinked and non-crosslinked films are very similar.

The three-dimensional AFM images of crosslinked EM films before and after aging under simulated weathering for 50 h are shown in Fig. 11. The surface of the pristine crosslinked EM base film is relatively smooth with an RMS roughness value of 0.92 nm (Fig. 11(a)), similar to that of

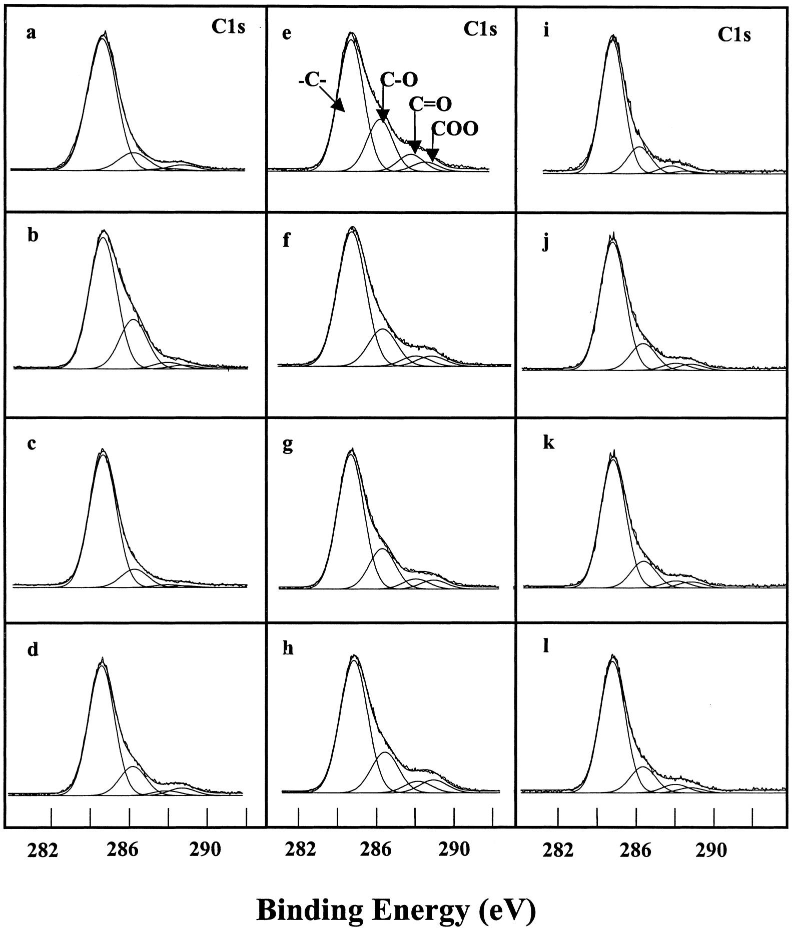

Fig. 10. XPS C1s core-level spectra of (a)–(d) crosslinked EM base film and the films reprotonated by $HClO_4$, TSA and SSA, respectively; (e)–(h) the respective films after simulated weathering (UV-vis + H_2O) for 50 h; (i)–(l) the respective films after UV-vis irradiation only for 50 h.

Table 4
Bulk composition of crosslinked films before and after simulated weathering (UV-vis + H_2O) and UV-vis irradiation (UV-vis)

Sample	Aging condition	Elemental composition		
		C/N	H/N	Cl or S/N
$HClO_4$-EM	Pristine	6.1	6.3	0.30
	UV-vis + H_2O, 50 h	6.0	5.9	0.13
	UV-vis, 50 h	5.9	5.6	0.21
TSA-EM	Pristine	6.0	5.5	0.011
	UV-vis + H_2O, 50 h	5.9	5.4	0.004
	UV-vis, 50 h	5.9	5.5	0.008
SSA-EM	Pristine	5.8	5.3	0
	UV-vis + H_2O, 50 h	5.9	5.4	0
	UV-vis, 50 h	5.8	5.3	0

the pristine non-crosslinked EM base film. However, the surface morphology of the crosslinked film is more resistant to change during simulated weathering for 50 h, with an increase in roughness to 2.53 nm (Fig. 11(b)), as compared to 4.58 for the non-crosslinked film. However, reprotonation of the crosslinked film by $HClO_4$ causes it to become significantly coarser with a roughness of 12.87 nm (Fig. 12(a)), and unlike the crosslinked base film, the surface morphology of the reprotonated film undergoes a drastic change after 50 h of simulated weathering to give rise to a surface roughness of 38.67 (Fig. 12(b)). It is possible that the relatively rough surface of the reprotonated crosslinked film compared to that of the reprotonated non-crosslinked film further enhances the surface reactions under simulated weathering by providing a larger specific surface area leading to the result shown in Fig. 12(b).

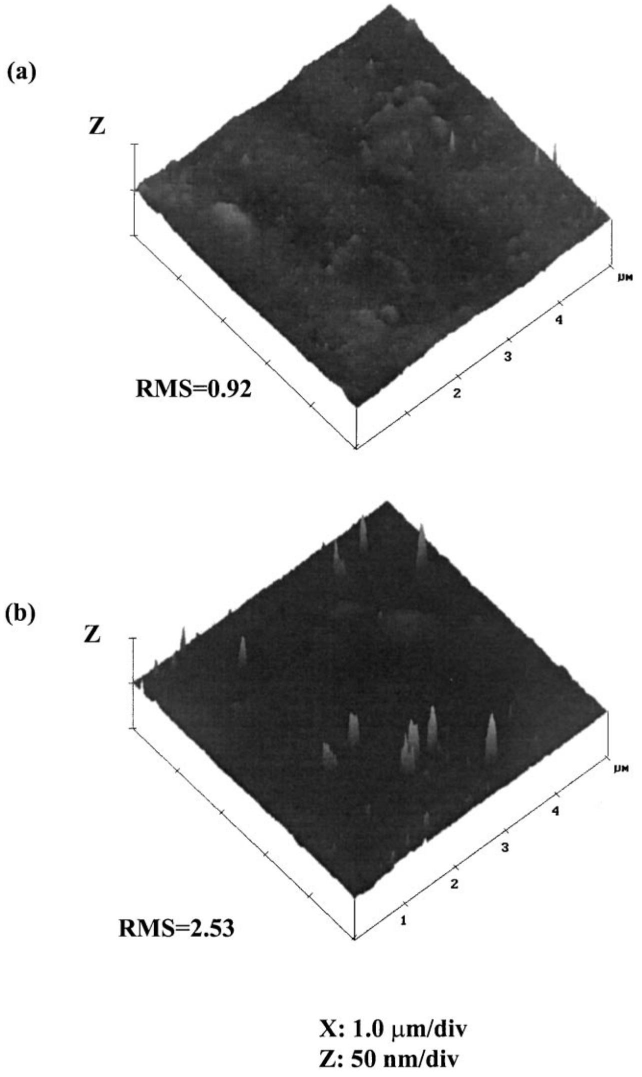

Fig. 11. AFM images of crosslinked EM film: (a) pristine and (b) after simulated weathering (UV-vis + H_2O) for 50 h.

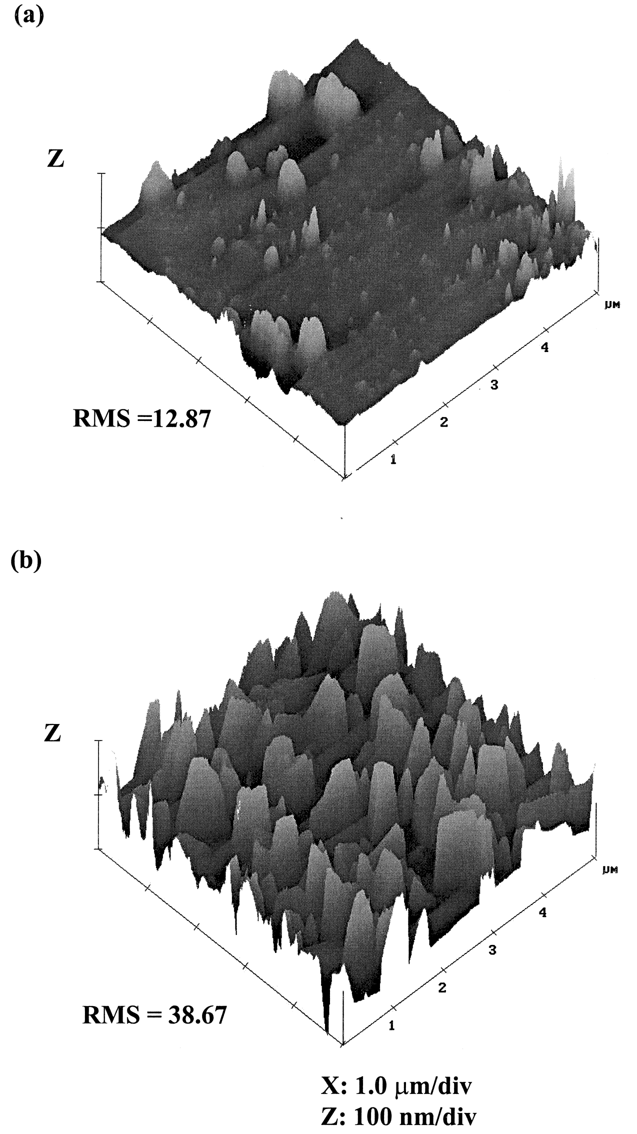

Fig. 12. AFM images of $HClO_4$-reprotonated crosslinked EM film: (a) pristine and (b) after simulated weathering (UV-vis + H_2O) for 50 h.

Under UV-visible irradiation only (without the activation of water spray), the resistivity of the crosslinked EM base film also remains unchanged (Fig. 7(b)), while the resistivity of the $HClO_4$-, TSA- and SSA-reprotonated crosslinked films undergoes a larger increase than those of the non-crosslinked films (comparing Fig. 7(b) with Fig. 1(b)). However, the tensile strength of all four types of crosslinked films show a much smaller change than those of the non-crosslinked counterparts (comparing Fig. 8(b) with Fig. 2(b)), suggesting that there is neither a substantial increase in crosslinking nor a degradation of the crosslinked structure in the former during this aging test. This is in contrast with the results obtained when the water spray is present during the UV-vis irradiation.

The greater change in resistivity of the crosslinked films after reprotonation compared to the non-crosslinked films under UV-visible irradiation is probably related to the greater loss of surface anions from the former (as can be seen from the anion/N ratios in Tables 1 and 3). The N1s and C1s core-level spectra of the crosslinked films after 50 h UV-vis irradiation are shown in Figs. 9(i)–(l) and 10(i)–(l), respectively. These spectra again represent an intermediate situation between those of the pristine films and the films after 50 h of simulated weathering in the presence of H_2O spray. The N^+/N ratios are significantly higher than the corresponding anion/N ratios, and this discrepancy is higher than that observed with the non-crosslinked films.

4. Conclusion

Solution-cast films of polyaniline were prepared with different degrees of crosslinking and these films were characterized by means of XPS, atomic force microscopy, bulk elemental analysis, resistivity and tensile strength measurements. The highly crosslinked film exhibits substantially higher (>50%) tensile strength but the migration of dopant anions into the bulk of the film during reprotonation is retarded, resulting in lowered electrical conductivity. Under simulated weathering involving UV-visible light irradiation with water spray, both the reprotonated non-crosslinked and crosslinked films exhibit an increase in tensile strength and resistivity as the dopant anions migrate out of the films. The resultant tensile strength may be higher than those of the pristine films before reprotonation and this effect is attributed to further crosslinking reactions. Under simulated weathering, the films undergo oxidation of the C ring, but the –N= species is reduced to the –NH– species. The surface roughness of the film also increases substantially and the effect is the greatest for reprotonated crosslinked films. The increase in surface roughness is attributed to the loss of NMP from the surface region of the film as well as the oxidation of the polymer backbone. The combined effect of UV-visible light irradiation and water spray greatly accelerates the degradation of the films compared to the effect of UV-visible light irradiation alone.

References

[1] MacDiarmid AG, Chiang JC, Richter AF, Epstein AJ. Synth Met 1987;18:285.
[2] Angelopoulous M, Asturias GE, Ermer SP, Ray A, Scherr EM, MacDiarmid AG. Mol Cryst Liq Cryst 1988;160:151.
[3] Fischer JE, Zhu Q, Tang X, Scherr EM, MacDiarmid AG, Cajipe VB. Macromolecules 1994;27:5094.
[4] Angelopoulos M, Ray A, MacDiarmid AG, Epstein AJ. Synth Met 1987;21:21.
[5] Cao Y, Smith P, Heeger AJ. Synth Met 1992;48:91.
[6] Tzou K, Gregory RV. Synth Met 1993;53:365.
[7] Neoh KG, Kang ET, Tan KL. Synth Met 1995;73:209.
[8] Kulkarni VG, Kampbell LD, Mathew WR. Synth Met 1989;30:321.
[9] Wang XH, Geng YH, Wang LX, Mathew WR. Synth Met 1989;30:321.
[10] Neoh KG, Kang ET, Tan KL. Polym Degrad Stab 1990;27:107.
[11] Thieblemount JC, Planche MF, Petrescu C, Bouvier JM, Bidan G. Synth Met 1993;59:81.
[12] Pyo M, Reynolds JR, Warren LFO, Marcy HO. Synth Met 1994;68:71.
[13] Yang CY, Reghu M, Heeger AJ, Cao Y. Synth Met 1996;79:27.
[14] Neoh KG, Kang ET, Tan KL. J Macromol Sci Chem 1992;A29:401.
[15] MacDiarmid AG, Min Y, Wiesinger JM, Oh EJ, Scherr EM, Epstein AJ. Synth Met 1993;55–57:753.
[16] Chen SA, Lee HT. Macromolecules 1993;26:3254.
[17] Kang ET, Neoh KG, Tan TC, Khor SH, Tan KL. Macromolecules 1990;23:2918.
[18] Tan KL, Tan BTG, Kang ET, Neoh KG. Phys Rev B 1989;39:8070.
[19] Kang ET, Neoh KG, Tan KL. Prog Polym Sci 1998;23:277.
[20] Neoh KG, Kang ET, Tan KL. J Phys Chem 1997;101:726.
[21] Li ZF, Kang ET, Neoh KG, Tan KL. Synth Met 1997;87:45.
[22] Neoh KG, Kang ET, Tan KL. J Phys Chem 1991;95:10 151.
[23] MacDiarmid AG, Yang LS, Huang WS, Humphrey BD. Synth Met 1987;18:393.
[24] Kang ET, Neoh KG, Woo YL, Tan KL, Huan CHA, Wee ATS. Synth Met 1993;53:333.
[25] Neoh KG, Kang ET, Tan KL. Polym Deg Stab 1994;43:141.
[26] Kang ET, Neoh KG, Zhang X, Tan KL, Liaw DJ. Surf Interf Anal 1996;24:51.
[27] Schoch KF, Byers Jr WA , Buckley LJ. Synth Met 1995;72:13.